Check for updates

AGU ADVANCING EARTH AND SPACE SCIENCES

Geophysical Research Letters

RESEARCH LETTER
10.1029/2024GL108609

Observation of Io's Resurfacing via Plume Deposition Using Ground-Based Adaptive Optics at Visible Wavelengths With LBT SHARK-VIS

Al Conrad[1], Fernando Pedichini[2,3], Gianluca Li Causi[2,3], Simone Antoniucci[2,3], Imke de Pater[4], Ashley Gerard Davies[5], Katherine de Kleer[6], Roberto Piazzesi[2,3], Vincenzo Testa[2,3], Piero Vaccari[2,3], Martina Vicinanza[2], Jennifer Power[1], Steve Ertel[1,7], Joseph C. Shields[1], Sam Ragland[1], Fabrizio Giorgi[2,3], Stuart M. Jefferies[8], Douglas Hope[9], Jason Perry[10], David A. Williams[11], and David M. Nelson[11]

[1]Large Binocular Telescope Observatory, The University of Arizona, Tucson, AZ, USA, [2]INAF Osservatorio Astronomico di Roma, Monte Porzio Catone, Italy, [3]INAF-ADONI, Adaptive Optics National Laboratory, Rome, Italy, [4]University of California—Berkeley, Berkeley, CA, USA, [5]Jet Propulsion Laboratory, California Institute of Technology, Pasadena, CA, USA, [6]California Institute of Technology, Pasadena, CA, USA, [7]Department of Astronomy and Steward Observatory, The University of Arizona, Tucson, AZ, USA, [8]Department of Physics and Astronomy, Georgia State University, Atlanta, GA, USA, [9]Georgia Tech Research Institute, Atlanta, GA, USA, [10]University of Arizona, 1200 E University Blvd, Tucson, AZ, USA, [11]Arizona State University, Tempe, AZ, USA

Key Points:

- High resolution images taken with SHARK-VIS at LBT reveal low and high albedo features obscuring a portion of Pele's red ring on Io
- This new eruption deposit likely originated from a powerful eruption in August 2021 located at Pillan Patera
- Such images provide a new imaging capability that yields vital context to other observations of planetary surfaces

Correspondence to:

A. Conrad,
aconrad@lbto.org

Citation:

Conrad, A., Pedichini, F., Li Causi, G., Antoniucci, S., de Pater, I., Davies, A. G., et al. (2024). Observation of Io's resurfacing via plume deposition using ground-based adaptive optics at visible wavelengths with LBT SHARK-VIS. *Geophysical Research Letters*, *51*, e2024GL108609. https://doi.org/10.1029/2024GL108609

Received 2 FEB 2024
Accepted 12 MAY 2024
Corrected 20 JUN 2024

This article was corrected on 20 JUN 2024. See the end of the full text for details.

Abstract Since volcanic activity was first discovered on Io from *Voyager* images in 1979, changes on Io's surface have been monitored from both spacecraft and ground-based telescopes. Here, we present the highest spatial resolution images of Io ever obtained from a ground-based telescope. These images, acquired by the SHARK-VIS instrument on the Large Binocular Telescope, show evidence of a major resurfacing event on Io's trailing hemisphere. When compared to the most recent spacecraft images, the SHARK-VIS images show that a plume deposit from a powerful eruption at Pillan Patera has covered part of the long-lived Pele plume deposit. Although this type of resurfacing event may be common on Io, few have been detected due to the rarity of spacecraft visits and the previously low spatial resolution available from Earth-based telescopes. The SHARK-VIS instrument ushers in a new era of high resolution imaging of Io's surface using adaptive optics at visible wavelengths.

Plain Language Summary A new instrument, called SHARK-VIS, on the Large Binocular Telescope in Arizona, has obtained high spatial resolution, visible wavelength images of Io, the highly volcanic moon of Jupiter. Large multicolored plume deposits were imaged, revealing where the red deposit from a volcano named Pele was covered by another plume deposit from another volcano, named Pillan Patera, the site of a powerful eruption in 2021. SHARK-VIS ushers in a new age in planetary imaging.

1. Introduction

Io is a highly volcanic world which sometimes exhibits large-scale surface changes (Davies, 2007; de Pater et al., 2021; Lopes et al., 2023). Io's volcanism is driven by strong tidal heating, induced by the Laplace (4:2:1) orbital resonance among Io, Europa, and Ganymede (Peale et al., 1979). That Io is currently volcanically active was discovered by the imaging of giant volcanic plumes of gas and dust by *Voyager 1* (Morabito et al., 1979; Smith et al., 1979). Subsequently, hundreds of active volcanoes have been identified via thermal emission observed in the infrared, and through the presence of surface changes, like plume deposits, at visible wavelengths. Plume deposits around the larger volcanoes can produce large-scale, multicolored, albedo changes that dominate the local landscape. On occasion, it is only the presence of the deposits that reveal that an eruption had taken place. The large Pele-type plumes (McEwen & Soderblom, 1983) have a high exit velocity (>1 km/s), can reach heights of over 300 km, and are difficult to image directly. The deposits from this plume type are annular, can be over 1,000 km in diameter, and are red in color, the result of the presence of short-chain (S_3 and S_4) sulfur allotropes. As these allotropes change to yellow cyclo-octal (S_8) sulfur under Io surface conditions in a few months, these large plume deposits are therefore ephemeral, as has been seen at Surt (335°W, 42°N) and South of Karei (13°W, 12°S) (Davies, 2007; Geissler et al., 2004).

© 2024. The Author(s).
This is an open access article under the terms of the Creative Commons Attribution-NonCommercial-NoDerivs License, which permits use and distribution in any medium, provided the original work is properly cited, the use is non-commercial and no modifications or adaptations are made.

19448007, 2024, 11, Downloaded from https://agupubs.onlinelibrary.wiley.com/doi/10.1029/2024GL108609 by CochraneItalia, Wiley Online Library on [04/02/2025]. See the Terms and Conditions (https://onlinelibrary.wiley.com/terms-and-conditions) on Wiley Online Library for rules of use; OA articles are governed by the applicable Creative Commons License

An exception to the short-lived nature of the giant plume deposits is Pele. First observed by *Voyager 1* in 1979 (Smith et al., 1979), Pele's plume deposit is continually being renewed by degassing from a persistent lava lake (Davies et al., 2001) at 255.6°W, 18.4°S, a location on Io's trailing hemisphere. The resulting plume deposit is over 1,200 km across. Close to the center of the plume deposit, around the lava lake, darker material is deposited, likely clasts of silicate lava caught in the gas stream which detrain from the gas flow as the gases expand. The Pele lava lake at the center of the plume deposit is a long-lived thermal source, although it has diminished in strength over the past decade (Davies et al., 2001; de Kleer & Rathbun, 2023; de Pater et al., 2016). Whether the amount of material being ejected has also diminished in strength has been an unanswered question as the last time this area of Io was imaged at visible wavelengths was in 2007 by *New Horizons* (Spencer et al., 2007) (see also NASA Photojournal image PIA09355).

Notably, in 1997 during the *Galileo* mission, a dark, likely silicate-rich deposit with a relatively narrow, higher-albedo aureole originating from a nearby eruption at Pillan (245°W, 11°S) covered a portion of Pele's red ring. Over the next 4 years, instruments on *Galileo* watched as the thermal emission from the Pillan eruption waned (Davies et al., 2001) and the dark Pillan deposit was mostly erased by the continuing deposition of material from the Pele plume (Davies et al., 2001; Keszthelyi et al., 2001; Turtle et al., 2004).

Now, over 25 years later, a similar resurfacing event has been detected by SHARK-VIS (Pedichini et al., 2022) at the Large Binocular Telescope (LBT), one of the first visible light, diffraction limited imagers operating on an 8–10 m telescope in the Northern Hemisphere.

2. Observations

2.1. Adaptive Optics at Visible Wavelengths

Adaptive Optics (AO), the technology that employs a deformable mirror to compensate for atmospheric distortion, has been in use on large telescopes for over 25 years (Lai et al., 1997). Until recently, however, the science path for the system has been restricted almost exclusively to infrared wavelengths. Thanks largely to two emerging technologies, high density deformable mirrors and fast visible light detectors with low read out noise, a higher resolution era is emerging for large telescopes equipped with imagers optimized for visible AO.

While there will always be a need for infrared images of Io, particularly at L (3.8 μm) and at M (4.8 μm) bands, to detect thermal emission from active volcanoes, visible-light images are essential to "see" the landscape, that is, identify locations of eruptions and associated features such as plume deposits. As shown in this paper, such images can now be obtained at high spatial resolution from ground-based telescopes on Earth with a spatial resolution of approximately 80 km at 550 nm. Hitherto visible-light images could only be obtained by spacecraft, or with the Hubble Space Telescope (HST) (Spencer et al., 1997); the spatial resolution of the latter images are, however, roughly a factor of 3 lower than the images obtained with SHARK-VIS on the LBT, due to the difference in aperture size.

2.2. SHARK-VIS on the LBT

SHARK-VIS saw first light at LBT on 2 October 2023. The instrument shares the center-bent Gregorian focus on the right-hand (DX) side of the LBT with the Large Binocular Telescope Interferometer (Ertel et al., 2020; Hinz et al., 2016), where it picks up the visible light from the direct beam using a deployable dichroic. The remaining red-visible and infrared light is transmitted to the LBTI and the shared wavefront sensor (Bailey et al., 2014) which has recently received the Single-conjugated adaptive Optics Upgrade for the LBT (Pinna et al., 2016). SHARK-VIS is an imager operating in the 400–1,000 nm wavelength range and delivers spatial resolutions down to ∼15 mas (at 550 nm), which in the infrared bands will be achieved only by future extremely large telescopes (ELTs). With a plate scale of 6.5 mas/pixel, SHARK-VIS provides slight oversampling of the Nyquist frequency for this resolution.

The spatial resolution given above (∼15 mas at 550 nm), is computed as follows: The entrance pupil of the AO system reduces the 8.4 m LBT aperture to 8.25 m. The full width half max (FWHM) of the Airy disk is then $1.03 \times \lambda/D = 14.2$ (∼15) mas for $\lambda = 550$ nm.

19448007, 2024, 11, Downloaded from https://agupubs.onlinelibrary.wiley.com/doi/10.1029/2024GL108609 by CochraneItalia, Wiley Online Library on [04/02/2025]. See the Terms and Conditions (https://onlinelibrary.wiley.com/terms-and-conditions) on Wiley Online Library for rules of use; OA articles are governed by the applicable Creative Commons License

Table 1
Observing Parameters for the LBT SHARK-VIS Observation of Io

UT	Filter	λ (nm)	No of frames[a]	Exposure time	
				Total (s)	Per frame (ms)
23 November 2023[b]:					
7 hr 11 min 16.5 s	V	495–605	1,000	10.0	10
7 hr 13 min 40.5 s	I	685–825	1,000	10.0	10
7 hr 16 min 00.5 s	R	552–687	1,000	10.0	10
10 January 2024[c]:					
2 hr 31 min 23:4 s	V	495–605	1,000	5.0	5
2 hr 30 min 48:3 s	I	685–825	1,000	5.0	5
2 hr 30 min 18:1 s	R	552–687	1,000	5.0	5

[a]Number of selected frames (using the criteria given in Section 2.3). The total number of frames collected were 12,000 and 24,000 for 23 November and 10 January, respectively. The Ephemerides are obtained from JPL's HORIZONS system: https://ssd.jpl.nasa.gov/horizons/app.html#/. [b]The observer-target (Δ) and heliocentric (r) distances; Io's diameter (D); the sub-observer W. longitude (λ_E) and latitude (θ_E); and the sub-solar W. longitude (λ_S) and sub-solar latitude (θ_S) are: $\Delta = 4.052$ AU, $r = 4.977$ AU, $D = 1.24''$, $\lambda_E \sim 264°$, $\theta_E = 3.30°$, $\lambda_S \sim 260°$, $\theta_S = 3.13°$. [c]$\Delta = 4.619$ AU, $r = 4.986$ AU, $D = 1.09''$, $\lambda_E \sim 273°$, $\theta_E = 3.03°$, $\lambda_S \sim 262°$, $\theta_S = 3.14°$.

The LBT AO system delivers this level of performance in ideal atmospheric conditions for targets within 40° of zenith (1.3 airmass or less). For the observations reported here, the achieved spatial resolution was ∼24 mas (as described in Section 2.4 below).

SHARK-VIS is equipped with an Andor Zyla 4.2 PLUS sCMOS science camera that can operate at a frame rate up to 1 Khz with a relatively low readout noise; this makes it possible to employ a fast imaging approach that helps freeze both atmospheric turbulence and telescope vibrations and allows for both post-facto registration and advanced processing of the frames with a significant improvement of the image sharpness (Hope et al., 2022; Pedichini et al., 2017; Stangalini et al., 2017). SHARK-VIS has a wide-band atmospheric dispersion corrector (ADC) enabling the use of 150 nm wide-band filters from 500 to 1,000 nm and 50 nm wide bands in the range 400–500 nm while covering zenith angles up to 40°.

2.3. Acquisition and Data Reduction

We observed Io with SHARK-VIS on UT 23rd November 2023 and UT 10th January 2024, taking data in each of 3 filters, as tabulated (together with the relevant ephemerides) in Table 1. Both November and January observations consisted of a sequence of 2 min of short exposures for each filter (10 and 5 ms), respectively, which were corrected for darks and the flat field. During processing, the frames were ranked for sharpness, based on the maximum spatial frequency above the noise level in the power spectra; the 1,000 best frames were selected, whose average UT is reported in Table 1. The frames were then de-rotated to sky orientation by correcting for the parallactic angle (due to the fact that SHARK-VIS does not have a mechanical de-rotator). As a final step, the center of the body was measured in each frame by fitting a circle to the object's limb, found as the maximum gradient locus in all directions from the image baricenter outwards, and the frames were co-registered via Fourier shifting, then average stacked, and finally oriented to have Io's North pole pointing upwards, based on JPL's HORIZONS ephemerides (https://ssd.jpl.nasa.gov/horizons/app.html#/). The resulting images are shown in the first two rows of Figure 1. The January images are more detailed, even though the apparent diameter of Io was larger in November. This is because, due to a technical problem, data collected during the November run suffered from an imperfect correction of non-common-path aberration by the AO system. The three filters were also combined to form the tri-color images shown in Figure 2, where the I, R, V bands have been rendered as RGB respectively. Image stretching and saturation have been slightly enhanced to improve the visibility of faint morphological structures on the satellite's surface. As a result of this processing, the colors produced are different from the colors seen in *Galileo* images (Figure 2 top center panel) and Voyager images, which were also not true color. The annular Pele plume deposit, however, still appears red in the SHARK-VIS images since it is less absorbing in the I-band (Figure 1).

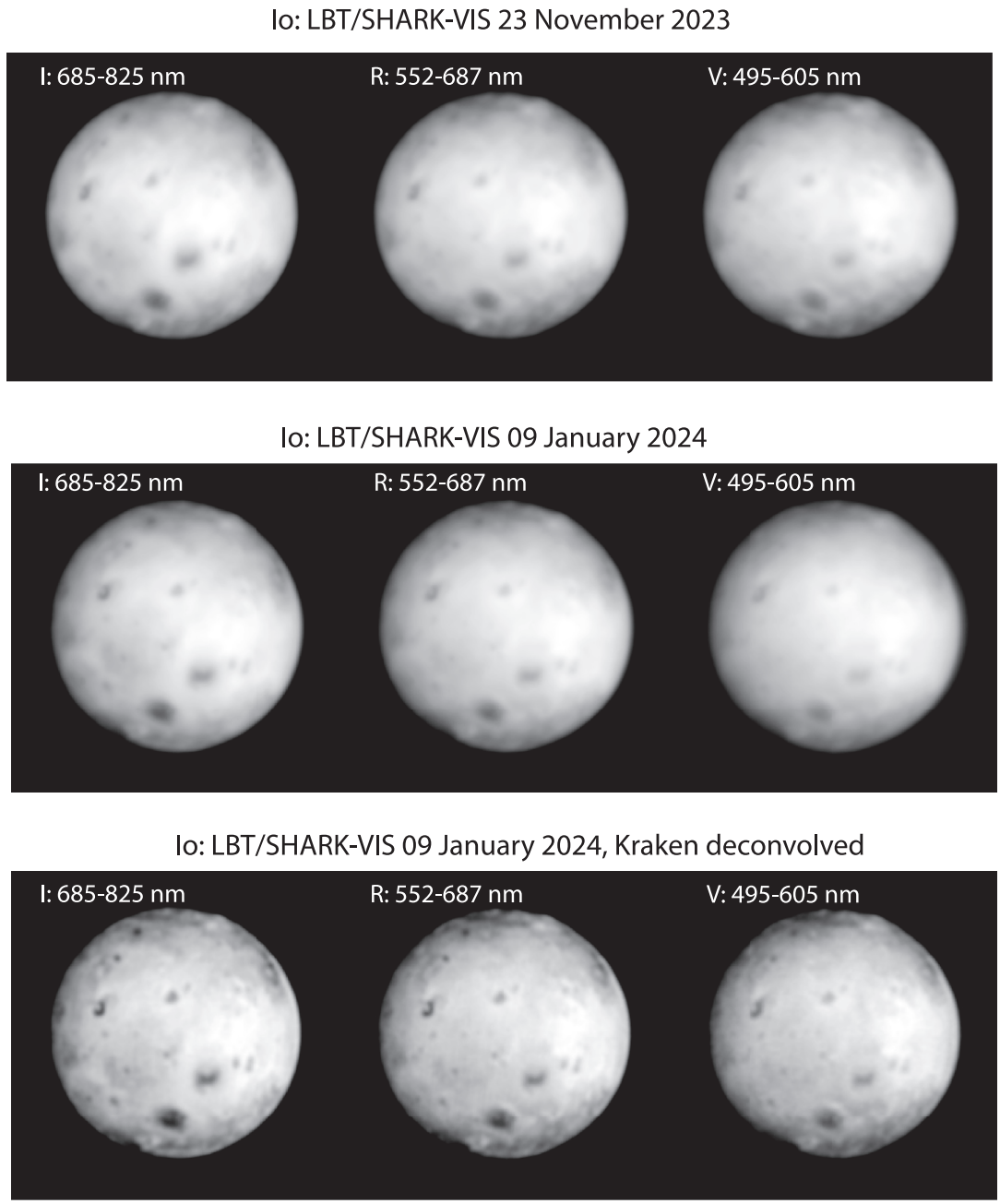

Figure 1. Images of Io obtained with SHARK-VIS on the LBT in November 2023 and January 2024. The images are re-scaled to Io's apparent diameter. The third row shows the Kraken deconvolved images from January 2024. The filter used is shown on each image. Io North is approximately up.

2.4. Multi-Frame Blind Deconvolution

A 5 ms frame sequence like that acquired from SHARK-VIS contains more information than can be retrieved by simple shift-and-add stacking. In fact, the frame-to-frame PSF diversity can be exploited to jointly estimate the instantaneous wavefront and reconstruct the brightness distribution of the object at a nearly diffraction limited resolution. To realize this approach, we applied Kraken multi-frame blind deconvolution (Hope et al., 2022; Leist et al., 2024) to the 250 sharpest frames of the January acquisition, which produced a much more detailed view of Io in all the three bands (Figure 1 bottom panel), and in the corresponding color composite (Figure 2 bottom left frame), at a FWHM resolution of 3.63 pixels (i.e., 24 mas for the plate scale of SHARK-VIS), as computed from

19448007, 2024, 11, Downloaded from https://agupubs.onlinelibrary.wiley.com/doi/10.1029/2024GL108609 by CochraneItalia, Wiley Online Library on [04/02/2025]. See the Terms and Conditions (https://onlinelibrary.wiley.com/terms-and-conditions) on Wiley Online Library for rules of use; OA articles are governed by the applicable Creative Commons License

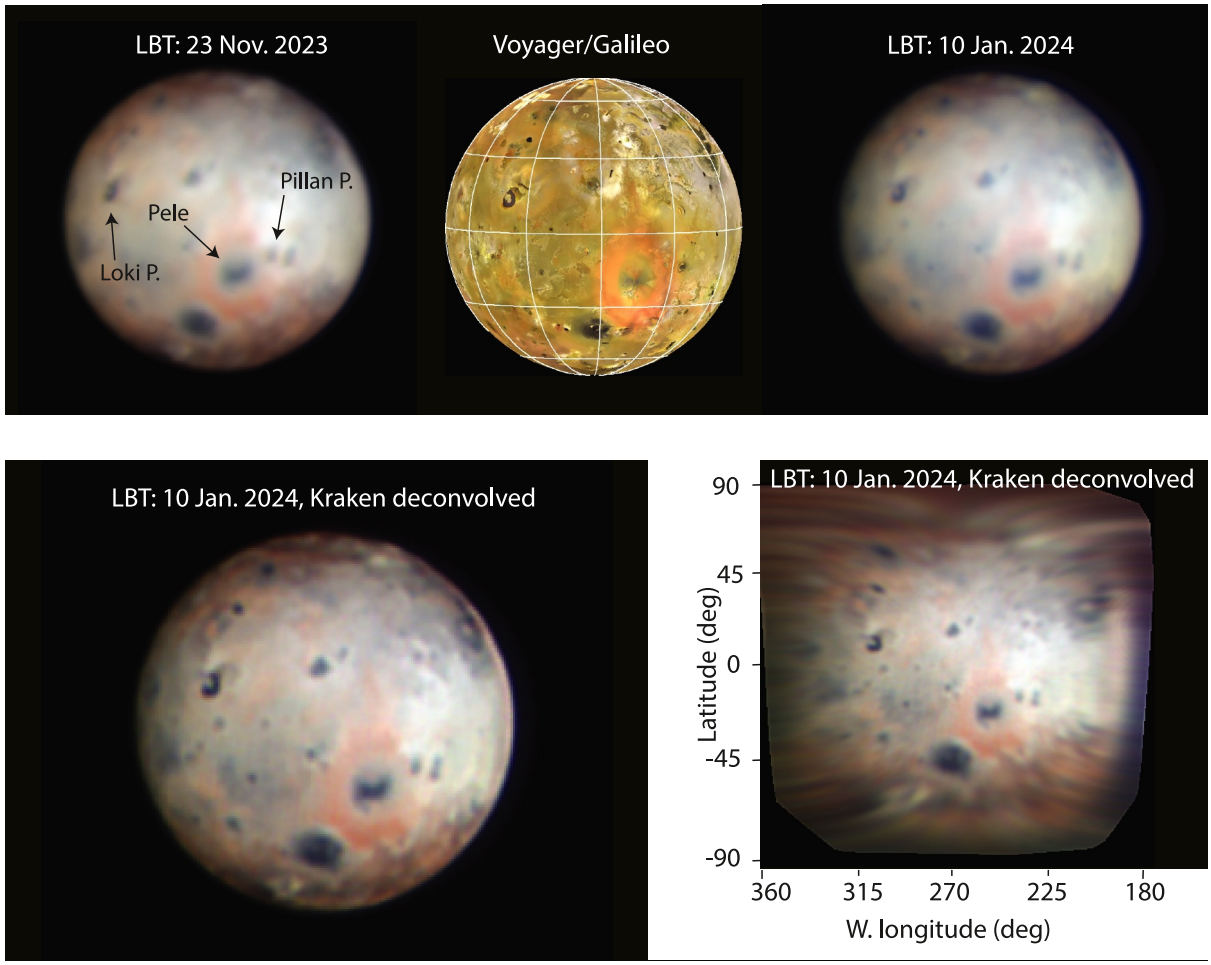

Figure 2. The SHARK-VIS detection image on 23 November 2023 (upper left), on 10 January 2024 (upper right), and the reprojection of the *Voyager* and *Galileo* spacecraft-derived Io photomosaic for 10 January 2024 (center) (Becker & Geissler, 2005). Labels to Pele, Pillan Patera and Loki Patera are shown on the upper left image. The bottom row shows the Kraken-deconvolved image from 10 January 2024 on the left; the bottom right map shows this image reprojected onto equirectangular (approximate) longitude-latitude coordinates. All images have been rotated so Io North is up. No detectable change to the Pillan plume deposit has occurred during the 50 days separating the two observations.

the maximum frequency of its power spectrum. For Io's distance in January (see Table 1), a single SHARK-VIS pixel spanned ∼22 km. The achieved spatial resolution on the surface of Io is therefore ∼80 km.

3. Results: A Resurfacing Event at Pillan Patera

As seen in the left- and right-hand panels of Figure 2, and with more details in the bottom panels, the red annular deposit centered on Pele is missing a segment. About $\frac{1}{4}$ of the ring is obscured by a high albedo deposit with a low albedo center. The bright deposit is likely SO_2 ice, which is ubiquitous on Io and a common component of volcanic plumes and plume deposits. The previous most recent high resolution visible imaging of the area was performed during an Io fly by by the *New Horizons* spacecraft in 2007 (see above), at which time the ring was intact. Additionally, there is a dark area centered on nearby Reiden Patera, another volcano active during the *Galileo* and *Juno* epochs (Davies et al., 2024; Veeder et al., 2015). Another dark area is seen at Ra Patera, the site of an extensive resurfacing event imaged by *Galileo* (Geissler et al., 2004). Ra Patera was imaged by JunoCam during *Juno* orbit PJ58 on 2 March 2024 (e.g., image JNCE_2024034_58C00026_V01). The patera exhibits a reddish rim and dark floor with associated extra-patera dark flows. Taken together, these dark features are consistent with the SHARK-VIS imagery. Such low albedo areas are expected from recent or ongoing silicate volcanism.

19448007, 2024, 11, Downloaded from https://agupubs.onlinelibrary.wiley.com/doi/10.1029/2024GL108609 by CochraneItalia, Wiley Online Library on [04/02/2025]. See the Terms and Conditions (https://onlinelibrary.wiley.com/terms-and-conditions) on Wiley Online Library for rules of use; OA articles are governed by the applicable Creative Commons License

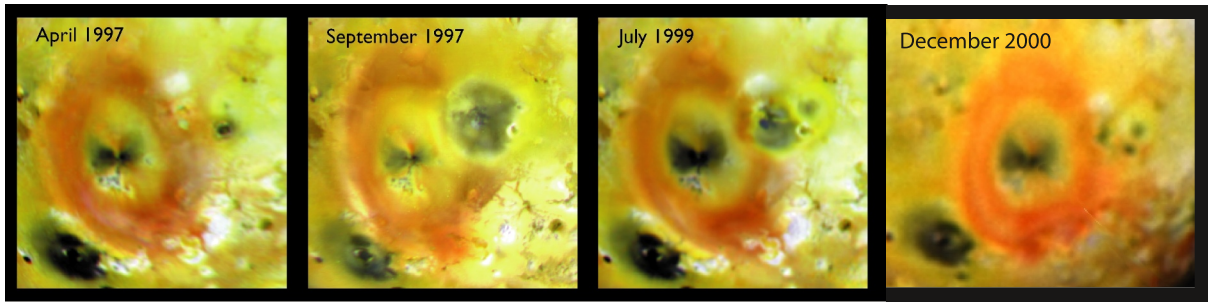

Figure 3. Four images following the 1997 Pillan eruption which show the plume deposit covering a portion of Pele's red ring for over 2 years. April 1997 (left): pre-eruption. September 1997 (middle left). The eruption may have started in May but only peaked in June (Davies et al., 2001), and then steadily decreased in thermal emission over the next few years. July 1999 (middle right): the Pele plume deposits had begun burying the Pillan deposits, but there is still evidence of an interaction between the Pele plume and degassing from the Pillan eruption site and/or emplaced flows. December 2000 (*Galileo* orbit 29): the Pele plume has completely recovered. (Image credits: both NASA/JPL/University of Arizona. The three left panels are from https://photojournal.jpl.nasa.gov/catalog/PIA02501. The right panel is from https://photojournal.jpl.nasa.gov/catalog/PIA02588).

The SHARK-VIS images of Pele and Pillan Patera are reminiscent of an image obtained in September 1997 by the Solid State Imaging experiment (SSI) (Belton et al., 1992) on the *Galileo* spacecraft, which showed that Pele's ring was partly covered by a plume deposit from a powerful, voluminous eruption originating to the northwest of Pillan Patera (see Figure 3) (Geissler et al., 2004). The Pele deposit had partially recovered by July 1999, slightly less than 2 years after the Pillan deposit formed. By late December 2000 the Pele plume deposit had completely recovered (Turtle et al., 2004).

The most likely source of the material that is covering the Pele plume deposit as seen in the SHARK-VIS images is another powerful eruption near Pillan Patera (244°W, 12°S, as indicated in Figure 2 upper left panel). In the following text we examine when such an eruption was most likely to have taken place.

Examination of observations of Io in the infrared from different observation systems, both telescopes (Gemini, Keck, IRTF) and spacecraft (*Juno*), allow a timeline of events to be compiled. Table 2 provides an eruption history for Pillan Patera spanning 3 years prior to, and just beyond, the SHARK-VIS detection. Keck and Gemini images documenting the non-detections in Table 2 are shown in Figure 4; the upper limit values are based upon prior observations with these instruments (de Kleer & de Pater, 2016; de Pater et al., 2016). Recent *Juno* JIRAM infrared data analysis shows 4.8-μm thermal emission from an active, volcanic source, albeit at a relatively low level (average 4.46 GW/μm), emanating from Pillan Patera (Davies et al., 2024). There are no other thermal sources detected by JIRAM between 2017 and early 2023 close to the location of the black deposit identified in Figure 2. On 13th August 2021, an extremely powerful eruption, designated as an "outburst" event, was detected at or near Pillan Patera by the InfraRed Telescope Facility (IRTF) (Tate et al., 2023). This eruption is the most likely source of the material that covers the Pele ring, and that is seen in the SHARK-VIS images 2 years later.

The IRTF images were obtained in L and M bands, where the thermal hot spot emission clearly stands out above the solar reflected light. Two weeks later, on August 27, the emission had subsided considerably (Tate et al., 2023), while 3 weeks earlier, on July 21, no emission was detected from Pillan Patera by the Keck telescope (see Figure 4). The event was not observed at its height by other groundbased telescopes nor by instruments on *Juno*, but is bracketed by both JIRAM and Keck observations. Also, the S+ torus and Na nebula seem quiescent during this event (Morgenthaler et al., 2024). The event in the Pillan Patera vicinity was powerful, but short-lived.

JunoCam, the visible wavelength imager on the *Juno* spacecraft (Hansen et al., 2017), has obtained a number of images of Io, mostly from a high-latitude, sub-spacecraft vantage point, and at moderate- to high-phase angles (Ravine et al., 2024). Observation opportunities are necessarily limited by the spacecraft trajectories, with *Juno* in a highly inclined orbit around Jupiter. While JunoCam has returned high spatial resolution images of mainly Io's northern hemisphere (https://www.missionjuno.swri.edu/junocam), it had not, at the time of the SHARK-VIS observations, imaged all of the Pele plume deposit. Coverage was limited to the western and northern portions of the plume deposit. As discussed below, on 9 April 2024 (PJ60) JunoCam did capture the entire Pele deposit; the combination of coverage from *Juno* and SHARK-VIS proving to be highly complementary.

19448007, 2024, 11, Downloaded from https://agupubs.onlinelibrary.wiley.com/doi/10.1029/2024GL108609 by CochraneItalia, Wiley Online Library on [04/02/2025]. See the Terms and Conditions (https://onlinelibrary.wiley.com/terms-and-conditions) on Wiley Online Library for rules of use; OA articles are governed by the applicable Creative Commons License

19448007, 2024, 11, Downloaded from https://agupubs.onlinelibrary.wiley.com/doi/10.1029/2024GL108609 by CochraneItalia, Wiley Online Library on [04/02/2025]. See the Terms and Conditions (https://onlinelibrary.wiley.com/terms-and-conditions) on Wiley Online Library for rules of use; OA articles are governed by the applicable Creative Commons License

Table 2
Observations of the Pillan Patera and Pele Regions From Early 2021 Through Early 2024, Encompassing the Major 2021 Eruption at Pillan Patera and the 2023-2024 SHARK-VIS Observations

Pillan, spectral radiance M-band, GW/μm	Pele, spectral radiance M-band, GW/μm	Date year month day	*Juno* orbit, or telescope
2.191	10.9	21 February 2021	PJ32i
3.364	11.7	15 April 2021	PJ33
<3	8.7 ± 1.5	21 July 2021	Keck
527 ± 118 L-band		13 August 2021	IRTF
Faint L-band, some M-band		27 August 2021	IRTF
>23.371	9.9	16 October 2021	PJ37i
<9 L-band	<9 L-band	15 December 2021	Gemini-N
16.537	10	24 February 2022	PJ40
<9 L-band	<9 L-band	01 June 2022	Gemini-N
<9 L-band	<9 L-band	06 June 2022	Gemini-N
<9 L-band	<9 L-band	08 June 2022	Gemini-N
8 ± 1	10 ± 1.5	16 August 2022	Keck
<3	Faint, on limb	02 December 2022	Keck
2.097		01 March 2023	PJ49
0.882	44	16 May 2023	PJ51
<4 L-band	5.2 ± 0.6 L-band	13 June 2023	Keck
<3	10.4 ± 1.5	18 June 2023	Keck
<3	14 ± 2	11 July 2023	Keck
<3	11 ± 1.4	12 August 2023	Keck
Visible wavelengths		23 November 2023	LBT/SHARK-VIS
<3	10 ± 2	23 December 2023	Keck
Visible wavelengths		24 January 2024	LBT/SHARK-VIS
JunoCam		09 April 2024	PJ60

Note. IRTF-derived spectral radiances are from Tate et al. (2023). Note that the positions in Tate et al. (2023) are ±10°. The thermal emission estimate for 2021 August 13 has been corrected for emission angle and converted to GW/μm. All Keck observations have been corrected for the emission angle. The data from *Juno* JIRAM are from Davies et al. (2024).

4. Discussion

The resurfacing scenario that occurred 25 years ago was likely similar to what took place recently, with some important changes. As seen with SHARK-VIS about 2 years after the Pillan outburst, the Pele plume deposit was not repaired as it was after the 1997 Pillan eruption. We note that the plume deposit restoration timeline depends on the effusive volcanic activity within Pillan Patera and the recent rate of degassing, the level of volcanic activity at Pele, and the continuation of sulfur supply to the Pele plume.

Assuming that the Pillan Patera plume deposit was likely initially laid down in August 2021 by the outburst eruption (see Table 2), the Pillan Patera eruption deposits persisted for at least 29 months (to January 2024). The plume deposit laid down in 1997 had mostly been buried after 2 years (Turtle et al., 2004). That the new deposit was apparently longer lasting than the 1997 deposit might be the result of less volcanic activity at Pele at present than during the *Galileo* era. The drop in activity manifested as a ∼75% drop in total thermal emission after the *Galileo* mission from 280 GW (Davies et al., 2001) to 60 GW (Davies et al., 2023; de Kleer & Rathbun, 2023; de Pater et al., 2016; Rathbun et al., 2014). A lower volumetric lava effusion rate might also suggest a similar decrease in gas emission volume (Davies, 2007). The plume resurfacing rate at Pele during the *Galileo* epoch was estimated at 0.6 mm/yr (Davies, 2007; Zhang et al., 2003), and may for recent years have been only a quarter of this.

However, a four-fold increase in thermal output from Pele was detected by JIRAM on 16 May 2023 during the *Juno* PJ51 flyby of Io. Both L-band and M-band spectral radiance from Pele exceeded 39 GW/μm, similar to

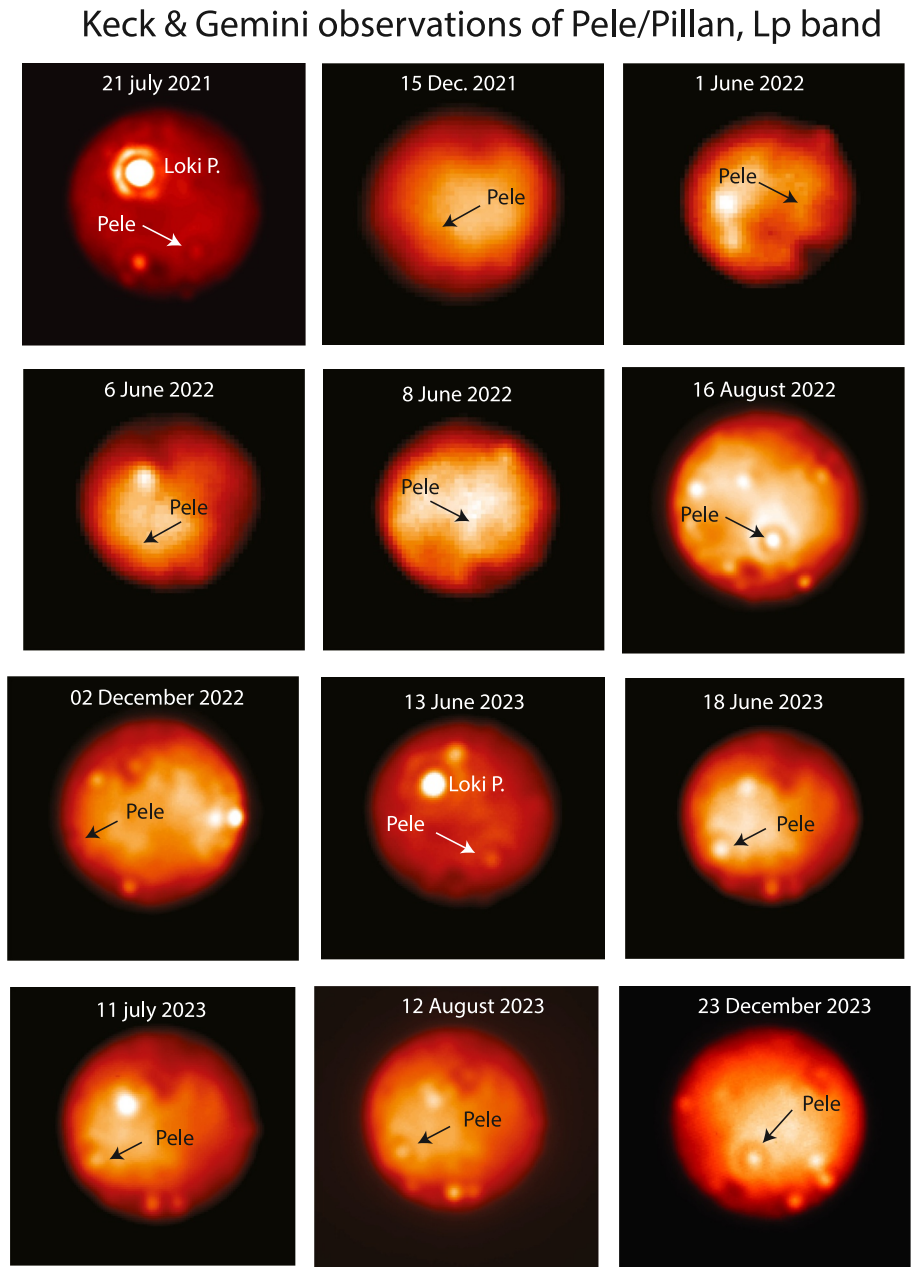

Figure 4. Keck and Gemini images of Io in Lp band (3.8 μm) of Pele/Pillan, which show no emission at Pillan Patera or the immediate surrounding area. Images from 15 December 2021 and from June 2022 are taken with the Gemini telescope. All other images are taken with the Keck telescope. Images from 2 December 2022, 13 and 18 June 2023 are from the Keck Twilight Zone website https://www2.keck.hawaii.edu/inst/tda/TwilightZone.html. All images have Io North up, and Pele has been indicated.

spectral radiance observed during the *Galileo* epoch, and suggesting a total thermal emission of 294 GW. Activity as seen by Keck and Gemini (Figure 4) then dropped, with Keck measuring a L-band spectral radiance of 5.2 ± 0.6 GW/μm on 13 June 2023, and 7 ± 0.8 GW/μm on 18 June 2023, with a M-band spectral radiance of 10.7 ± 1.5 GW/μm on the latter date. These numbers are typical for all Keck observations in Figure 4. Even with this apparent resurgence of activity at Pele (albeit temporary), the plume deposit was not restored in its entirety by the time of the SHARK-VIS observations.

If the deposits imaged by SHARK-VIS around Pillan Patera were indeed emplaced in 2021, then their persistence reveals a complex interplay of volcanic processes. As noted above, around the dark Pillan Patera deposit in the

19448007, 2024, 11, Downloaded from https://agupubs.onlinelibrary.wiley.com/doi/10.1029/2024GL108609 by CochraneItalia, Wiley Online Library on [04/02/2025]. See the Terms and Conditions (https://onlinelibrary.wiley.com/terms-and-conditions) on Wiley Online Library for rules of use; OA articles are governed by the applicable Creative Commons License

19448007, 2024, 11, Downloaded from https://agupubs.onlinelibrary.wiley.com/doi/10.1029/2024GL108609 by CochraneItalia, Wiley Online Library on [04/02/2025]. See the Terms and Conditions (https://onlinelibrary.wiley.com/terms-and-conditions) on Wiley Online Library for rules of use; OA articles are governed by the applicable Creative Commons License

SHARK-VIS images is a bright, high-albedo deposit (Figure 2), likely SO_2 frost. If the Io surface here is cold enough for SO_2 to condense it is also cold enough for plume sulfur to condense. As the rest of Pele plume deposit is seen, the plume must also be depositing material here, but it is not repairing the red ring. This suggests the presence of ongoing SO_2 deposition (the SO_2 originating from the Pillan Patera eruption) which is burying the Pele plume deposit faster than it is being emplaced, thus maintaining the gap in the ring seen by SHARK-VIS. The low albedo deposit centered on Pillan Patera persists probably because the deposition from Pele is landing on a warm, silicate-rich surface and is not condensing.

By early April 2024, however, the Pele ring appeared to have restored itself entirely. Observations obtained by JunoCam on 9 April 2024 during orbit PJ60, albeit at high emission angle (e.g., https://www.missionjuno.swri.edu/Vault/VaultOutput?VaultID=51967&ts=1709753150), cover just enough of Pele's deposit to suggest that the annular ring was once again complete. If this is the case, either SO_2 deposition from Pillan Patera significantly decreased or ceased entirely, or sulfur deposition from Pele increased enough to overwhelm any Pillan Patera deposition, allowing repair of the contiguous Pele plume deposit. The combination of coverage from *Juno* and SHARK-VIS are highly complementary. Without the SHARK-VIS images, this resurfacing event would never have been detected. With SHARK-VIS we now have the capability to regularly monitor the evolving plume deposits at Pele and Pillan Patera for years to come, as well as other such events on Io's surface. SHARK-VIS is available to researchers affiliated with one or more of the LBT member institutions (listed at the end of the *Acknowledgments* section below) and to other potential users via director's discretionary time.

5. Conclusions

SHARK-VIS ushers in a new era in planetary imaging. On its very first use imaging Io, SHARK-VIS observed a major change of volcanic origin on Io's surface, providing vital visual wavelength context for the interpretation of infrared and other observations by extending contemporaneous coverage of Io. With SHARK-VIS, we now have the capability to monitor how Io's surface changes and apply what is observed to better understand volcanic activity at Pele, Pillan, and elsewhere, with implications for the manner and rate of the resurfacing of Io.

Data Availability Statement

The data for this observation are recorded in FITS files as follows. These data are available from Zenodo (Conrad, 2024).

- For the November observation: 2023_11_22-IRV_centered.fits
- For the January observation: 2024_01_09-IRV_centered.fits

Acknowledgments
Observations have benefited from the use of ALTA Center (alta.arcetri.inaf.it) forecasts performed with the Astro-Meso-Nh model. Initialization data of the ALTA automatic forecast system come from the General Circulation Model (HRES) of the European Centre for Medium Range Weather Forecasts. The authors are grateful to Marco Stangalini for his help during the development of the Forerunner of SHARK-VIS and his suggestions about the fast imaging approach with sCMOS detectors. The Kraken code was developed under the Air Force Office of Scientific Research award number FA9550-14-1-0178. We thank the Keck Observatory staff for their dedication to obtaining Twilight Zone images. We acknowledge the vital work of the *Juno* Project in obtaining Io data. Part of this work was performed at the Jet Propulsion Laboratory—California Institute of Technology, under Government contract. Ashley Davies, Jason Perry, David Williams, and David Nelson are supported by the NASA New Frontiers Data Analysis Program (NFDAP) under award 80NM0018F0612. The LBT is an international collaboration among institutions in the United States, Italy, and Germany. LBT Corporation Members are: The University of Arizona on behalf of the Arizona Board of Regents; Istituto Nazionale di Astrofisica, Italy; LBT Beteiligungsgesellschaft, Germany, representing the Max-Planck Society, The Leibniz Institute for Astrophysics Potsdam, and Heidelberg University; The Ohio State University, representing OSU, University of Notre Dame, University of Minnesota and University of Virginia.

References

Bailey, V. P., Hinz, P. M., Puglisi, A. T., Esposito, S., Vaitheeswaran, V., Skemer, A. J., et al. (2014). Large binocular telescope interferometer adaptive optics: On-sky performance and lessons learned. In E. Marchetti, L. M. Close, & J.-P. Vran (Eds.), *Adaptive optics systems IV* (Vol. 9148, p. 914803). SPIE. https://doi.org/10.1117/12.2057138

Becker, T., & Geissler, P. E. (2005). *Galileo* global color Mosaics of Io. In *Lunar and planetary science conference* (Vol. 36). Abstract 1862.

Belton, M. J. S., Klaasen, K. P., Clary, M. C., Anderson, J. L., Anger, C. D., Carr, M. H., et al. (1992). The *Galileo* solid-state imaging experiment. *Space Science Reviews*, *60*(1–4), 413–455. https://doi.org/10.1007/BF00216864

Conrad, A. (2024). aconrad6962/svio2024: Shark-vis io data [Dataset]. https://zenodo.org/records/11493933/latest

Davies, A. G. (2007). *Volcanism on Io: A comparison with Earth* (p. 372). Cambridge University Press. https://doi.org/10.1017/CBO9781107279902

Davies, A. G., Keszthelyi, L. P., Williams, D. A., Phillips, C. B., McEwen, A. S., Lopes, R. M. C., et al. (2001). Thermal signature, eruption style, and eruption evolution at Pele and Pillan on Io. *Journal of Geophysical Research*, *106*(E12), 33079–33104. https://doi.org/10.1029/2000JE001357

Davies, A. G., Perry, J., Williams, D. A., & Nelson, D. M. (2023). Modelling Io's polar volcanic thermal emission using *Juno* JIRAM data. In *Lunar and planetary science conference* (Vol. 54). Abstract 2544.

Davies, A. G., Perry, J., Williams, D. A., & Nelson, D. M. (2024). Io's polar volcanic thermal emission indicative of magma ocean and shallow tidal heating models. *Nature Astronomy*, *8*(1), 94–100. https://doi.org/10.1038/s41550-023-02123-5

de Kleer, K., & de Pater, I. (2016). Time variability of Io's volcanic activity from near-IR adaptive optics observations on 100 nights in 2013-2015. *Icarus*, *280*, 378–404. https://doi.org/10.1016/j.icarus.2016.06.019

de Kleer, K., & Rathbun, J. (2023). Io's thermal emission and heat flow. In *Io: A new view of Jupiter's Moon*.

de Pater, I., Keane, J. T., de Kleer, K., & Davies, A. G. (2021). A 2020 observational perspective of Io. *Annual Review of Earth and Planetary Sciences*, *49*(1), 643–678. https://doi.org/10.1146/annurev-earth-082420-095244

de Pater, I., Laver, C., Davies, A. G., de Kleer, K., Williams, D. A., Howell, R. R., et al. (2016). Io: Eruptions at Pillan, and the time evolution of Pele and Pillan from 1996 to 2015. *Icarus*, *264*, 198–212. https://doi.org/10.1016/j.icarus.2015.09.006

Ertel, S., Hinz, P. M., Stone, J. M., Vaz, A., Montoya, O. M., West, G. S., et al. (2020). Overview and prospects of the LBTI beyond the completed HOSTS survey. In P. G. Tuthill, A. Mérand, & S. Sallum (Eds.), *Optical and infrared interferometry and imaging VII* (Vol. 11446, p. 1144607). https://doi.org/10.1117/12.2561849

Geissler, P., McEwen, A., Phillips, C., Keszthelyi, L., & Spencer, J. (2004). Surface changes on Io during the *Galileo* mission. *Icarus*, *169*(1), 29–64. https://doi.org/10.1016/j.icarus.2003.09.024

Hansen, C. J., Caplinger, M. A., Ingersoll, A., Ravine, M. A., Jensen, E., Bolton, S., & Orton, G. (2017). Junocam: *Juno*'s outreach camera. *Space Science Reviews*, *213*(1–4), 475–506. https://doi.org/10.1007/s11214-014-0079-x

Hinz, P. M., Defrère, D., Skemer, A., Bailey, V., Stone, J., Spalding, E., et al. (2016). Overview of LBTI: A multipurpose facility for high spatial resolution observations. In F. Malbet, M. J. Creech-Eakman, & P. G. Tuthill (Eds.), *Optical and infrared interferometry and imaging V* (Vol. 9907, p. 990704). SPIE. https://doi.org/10.1117/12.2233795

Hope, D. A., Jefferies, S. M., Li Causi, G., Landoni, M., Stangalini, M., Pedichini, F., & Antoniucci, S. (2022). Post-AO high-resolution imaging using the Kraken multi-frame blind deconvolution algorithm. *The Astrophysical Journal*, *926*(1), 88. https://doi.org/10.3847/1538-4357/ac2df3

Keszthelyi, L., McEwen, A. S., Phillips, C. B., Milazzo, M., Geissler, P., Turtle, E. P., et al. (2001). Imaging of volcanic activity on Jupiter's moon Io by *Galileo* during the *Galileo* Europa Mission and the *Galileo* Millennium Mission. *Journal of Geophysical Research*, *106*(E12), 33025–33052. https://doi.org/10.1029/2000je001383

Lai, O., Veran, J.-P., Rigaut, F. J., Rouan, D., Gigan, P., Lacombe, F., et al. (1997). CFHT adaptive optics: First results at the telescope. In A. L. Ardeberg (Ed.), *Optical telescopes of today and tomorrow* (Vol. 2871, pp. 859–870). SPIE. https://doi.org/10.1117/12.269121

Leist, M. T., Packham, C., Rosario, D. J. V., Hope, D. A., Alonso-Herrero, A., Hicks, E. K. S., et al. (2024). Deconvolution of JWST/MIRI images: Applications to an active galactic nucleus model and GATOS observations of NGC 5728. *The Astronomical Journal*, *167*(3), 96. https://doi.org/10.3847/1538-3881/ad1886

Lopes, R. M. C., de Kleer, K., & Keane, J. T. (2023). *Io: A new view of Jupiter's Moon* (p. 375). Springer.

McEwen, A. S., & Soderblom, L. A. (1983). Two classes of volcanic plumes on Io. *Icarus*, *55*(2), 191–217. https://doi.org/10.1016/0019-1035(83)90075-1

Morabito, L. A., Synnott, P. N., Kupferman, P. N., & Collins, S. A. (1979). Discovery of currently active extraterrestrial volcanism. *Science*, *204*(4396), 972. https://doi.org/10.1126/science.204.4396.972.a

Morgenthaler, J. P., Schmidt, C. A., Vogt, M. F., Schneider, N. M., & Marconi, M. (2024). Jovian sodium nebula and Io plasma torus S^+ and brightnesses 2017-2023: Insights into volcanic versus sublimation supply. *Journal of Geophysical Research: Space Physics*, *129*(3), e2023JA032081. https://doi.org/10.1029/2023JA032081

Peale, S. J., Cassen, P., & Reynolds, R. T. (1979). Melting of Io by tidal dissipation. *Science*, *203*(4383), 892–894. https://doi.org/10.1126/science.203.4383.892

Pedichini, F., Piazzesi, R., Viavattene, G., Antoniucci, S., Gangi, M., Li Causi, G., et al. (2022). SHARK-VIS ready for the stars: Instrument description and final laboratory performance test. In L. Schreiber, D. Schmidt, & E. Vernet (Eds.), *Adaptive optics systems VIII* (Vol. 12185, p. 121856Q). https://doi.org/10.1117/12.2629244

Pedichini, F., Stangalini, M., Ambrosino, F., Puglisi, A., Pinna, E., Bailey, V., et al. (2017). High contrast imaging in the visible: First experimental results at the large binocular telescope. *The Astronomical Journal*, *154*(2), 74. https://doi.org/10.3847/1538-3881/aa7ff3

Pinna, E., Esposito, S., Hinz, P., Agapito, G., Bonaglia, M., Puglisi, A., et al. (2016). SOUL: The single conjugated adaptive optics upgrade for LBT. In *Adaptive Optics Systems V*, E. Marchetti, L. M. Close, & J.-P. Véran (Eds.), (Vol. 9909, p. 99093V). https://doi.org/10.1117/12.2234444

Rathbun, J., Spencer, J., Lopes, R., & Howell, R. (2014). Io's active volcanoes during the *New Horizons* era: Insights from *New Horizons* imaging. *Icarus*, *231*, 261–272. https://doi.org/10.1016/j.icarus.2013.12.002

Ravine, M. A., Hansen, C. J., Caplinger, M. A., Schenk, P. M., Lipkaman Vittling, L., Krysak, D. J., et al. (2024). JunoCam images of Io. In *Lunar and planetary science conference*. Abstract 1718.

Smith, B. A., Soderblom, L. A., Johnson, T. V., Ingersoll, A. P., Collins, S. A., Shoemaker, E. M., et al. (1979). The Jupiter system through the eyes of *Voyager 1*. *Science*, *204*(4396), 1422–1449. https://doi.org/10.1126/science.204.4396.951

Spencer, J., Stern, S., Cheng, A., Weaver, H., Reuter, D., Retherford, K., et al. (2007). Io volcanism seen by *New Horizons*: A major eruption of the Tvashtar volcano. *Science*, *318*(5848), 240–243. https://doi.org/10.1126/science.1147621

Spencer, J. R., Sartoretti, P., Ballester, G. E., McEwen, A. S., Clarke, J. T., & McGrath, M. A. (1997). The Pele plume (Io): Observations with the Hubble Space Telescope. *Geophysical Research Letters*, *24*(20), 2471–2474. https://doi.org/10.1029/97GL02592

Stangalini, M., Pedichini, F., Pinna, E., Christou, J., Hill, J., Puglisi, A., et al. (2017). Speckle statistics in adaptive optics images at visible wavelengths. *Journal of Astronomical Telescopes, Instruments, and Systems*, *3*(2), 025001. https://doi.org/10.1117/1.JATIS.3.2.025001

Tate, C. D., Rathbun, J. A., Hayes, A. G., Spencer, J. R., & Pettine, M. (2023). Discovery of seven volcanic outbursts on Io from an infrared telescope facility observation campaign, 2016-2022. *Planetary Science Journal*, *4*(10), 189. https://doi.org/10.3847/PSJ/acf57e

Turtle, E. P., Keszthelyi, L. P., McEwen, A. S., Radebaugh, J., Milazzo, M., Simonelli, D. P., et al. (2004). The final *Galileo* SSI observations of Io: Orbits G28-I33. *Icarus*, *169*(1), 3–28. https://doi.org/10.1016/j.icarus.2003.10.014

Veeder, G. J., Davies, A. G., Matson, D. L., Johnson, T. V., Williams, D. A., & Radebaugh, J. (2015). Io: Heat flow from small volcanic features. *Icarus*, *245*, 379–410. https://doi.org/10.1016/j.icarus.2014.07.028

Zhang, J., Goldstein, D. B., Varghese, P. L., Gimelshein, N., Gimelshein, S., & Levin, D. (2003). Simulation of gas dynamics and radiation in volcanic plumes on Io. *Icarus*, *163*(1), 182–197. https://doi.org/10.1016/s0019-1035(03)00050-2

Erratum

The originally published version of this article contained an error. In Conrad, A. (2024), the URL "https://doi.org/10.5281/zenodo.11194341" has been updated with the following URL: "https://zenodo.org/records/11493933/latest." This may be considered the authoritative version of record.

19448007, 2024, 11, Downloaded from https://agupubs.onlinelibrary.wiley.com/doi/10.1029/2024GL108609 by CochraneItalia, Wiley Online Library on [04/02/2025]. See the Terms and Conditions (https://onlinelibrary.wiley.com/terms-and-conditions) on Wiley Online Library for rules of use; OA articles are governed by the applicable Creative Commons License